Original article

Jure Žigon*, Matjaž Pavlič, Pierre Kibleur, Jan Van den Bulcke, Marko Petrič, Joris Van Acker and Sebastian Dahle

Treatment of wood with atmospheric plasma discharge: study of the treatment process, dynamic wettability and interactions with a waterborne coating

https://doi.org/10.1515/hf-2020-0182
Received July 22, 2020; accepted November 3, 2020; published online December 10, 2020

Abstract: Plasma treatment is becoming a mature technique for modification of surfaces of various materials, including wood. A better insight in the treatment process and the impact of the plasma on properties of wood bulk are still needed. The study was performed on Norway spruce and common beech wood, as well as their thermally modified variations. The formations of the airborne discharge, as well as mass changes of the treated wood, were monitored. The impact of such treatment on wood-coating interaction was investigated by evaluating the dynamic wettability and penetration into wood. At the wood surface, plasma streamers were observed more intense on denser latewood regions. Wood mass loss was higher with increasing number of passes through the plasma discharge and was lower for thermally modified wood than for unmodified wood. Plasma treatment increased the surface free energy of all wood species and lowered the contact angles of a waterborne coating, these together indicating enhanced wettability after treatment. Finally, the distribution and penetration depth of the coating were studied with X-ray microtomography. It was found that the coating penetrated deeper into beech than into spruce wood. However, the treatment with plasma increased the penetration of the coating only into spruce wood.

Keywords: beech; coatings; plasma; spruce; wettability; wood.

***Corresponding author: Jure Žigon**, Department of Wood Science and Technology, Biotechnical Faculty, University of Ljubljana, Jamnikarjeva ulica 101, 1000, Ljubljana, Slovenia, E-mail: jure.zigon@bf.uni-lj.si
Matjaž Pavlič, Marko Petrič and Sebastian Dahle, Department of Wood Science and Technology, Biotechnical Faculty, University of Ljubljana, Jamnikarjeva ulica 101, 1000, Ljubljana, Slovenia. https://orcid.org/0000-0001-7568-0483 (S. Dahle)
Pierre Kibleur, Jan Van den Bulcke and Joris Van Acker, UGCT – UGent-Woodlab, Laboratory of Wood Technology, Department of Environment, Faculty of Bioscience Engineering, Ghent University, Coupure Links 653, 9000, Gent, Belgium

1 Introduction

In various conditions, wooden products may require the application of coatings to protect the substrate, change its visual appearance, or both. Coated wood can be divided into coating, a transfer region we call the wood-coating interface with a certain thickness, and wood. Together, they define the surface system (Liptáková et al. 2000; Liptáková and Kudelá 2003; Ma et al. 2013). The initial interaction between the wooden surface and the coating defines the durability of the surface system during later exposure to the environment. In the early stages of the formation of this protective layer, the most important factors for its durability are sufficient wettability of the wood surface, and spreading and penetration of the liquid coating (Bessières et al. 2013; Shi and Gardner 2001).

Among wood modification methods to protect the wood, thermal modification (Welzbacher and Scheiding 2011) can be performed by exposing wood to temperatures between 200 and 260 °C, in an inert atmosphere, at atmospheric (Esteves et al. 2008) or reduced pressures (Humar et al. 2017; Surini et al. 2012). This causes a loss of hydroxyl groups in lignin and hemicelluloses, which lowers both the dispersion and polar components of the surface free energy (SFE) (Gérardin et al. 2007; Petrič et al. 2007; Petrič et al. 2013). In turn, this makes the wood turn dark brown and more hydrophobic (Tjeerdsma et al. 1998). During this modification, volatile gases are generated, accompanied by a loss in mass and cross-section dimensions of the treated sample (Frangi and Fontana 2003). Thermally modified (TM) wood is currently well-known and widely

used due to its appearance, better dimensional stability, and resistance to insects and fungi (Willems et al. 2015). However, enhanced hydrophobicity of TM wood adversely affects its compatibility with waterborne finishes and adhesives (Kutnar et al. 2013; Pétrissans et al. 2003).

Among the techniques for modifying wood surfaces, plasma treatment (PT) is a rapidly developing surface treatment technology (Žigon et al. 2018). By avoiding volatile organic compounds and organic solvents, it is an environmentally friendly technique, which is also applicable to woody materials (Köhler et al. 2019). Plasma contains a large number of active species such as excited ions, molecules, photons and radicals, with energy sufficient to break typical chemical bonds on the surface of wood. Flux of these active species induce and promote chemical reactions on the treated surfaces (Sun et al. 2009). Such chemical activation is an effective way to attach polar or oxygen-containing functional groups to wood surfaces (Gramlich et al. 2006). However, not all wooden or cellulosic materials can be treated equally well with plasma (Gospodinova and Dineff 2019). It is well-known that water molecules in wood have an effect on the plasma stability and uniformity (Setoyama 1996).The wooden substrate having a given moisture content (MC), can act as an electrical conductor (Custódio et al. 2008; Rehn et al. 2003). Higher proportion of condensed and more hydrophobic lignin content by TM wood makes it well-suited for PT (Wolkenhauer et al. 2009a; Wolkenhauer et al. 2009b). Therefore, PT is a useful technique to make surfaces of wood more hydrophilic (Altgen et al. 2016), or for improving the bonding performance of wood (Lütkemeier et al. 2016) by the increment of the polar component of the SFE (Galmiz et al. 2019). Talviste et al. (2019) suggest a linear correlation between the SFE and the proportion of oxygen and carbon on the surface of the TM wood, before and after PT. When exposing wood to plasma, primarily the cellulose and hemicelluloses are degraded, while lignin is much less affected. After longer treatment periods (1, 3 or 5 min), nano-scale structures are formed on the surface. In that case, even etching and carving can be detected on the plasma-treated (PTd) wood surface (Galmiz et al. 2019; Jamali and Evans 2011). For surface processing, such changes are beneficial to the spreading, wetting, adsorption, penetration and adhesion of waterborne paints on the material surface (Peng and Zhang 2020). Unfortunately, the enhanced hydrophilicity resulting from PT is not permanent (Altgen et al. 2020; Novák et al. 2019; Odrášková et al. 2008).

Wettability measurements with various probe liquids enable to quantify the wettability of wood surfaces with coatings and glues alike (Hakkou et al. 2005; Petrič et al. 2013; Wålinder and Gardner 1999). When studying the interface between wood and coating, two basic systems are to be considered: the interface between a solid and a liquid (1), and the interface of two solids with different physical and chemical properties (2) (Liptáková et al. 2000). Dynamic contact angle (CA) analysis of liquids on the surface of wood can be performed by a variation of the Wilhelmy plate method (Mantanis and Young 1997; Wålinder 2002; Wilhelmy 1863). In general, this method relies on balancing the surface tension, gravity, and buoyancy acting on a thin plate, which is suspended vertically in the air-liquid interface (Lapham et al. 1999). Further details can be found in the works of Ramé (1997).

Beside the liquid properties, immersion speed and calculation method, the complex nature of wood can influence the calculated SFE (apparent SFE), which conditions the wettability. Density, porosity, grain direction, surface roughness, chemical heterogeneity, MC, polarity, capillary flow and the adsorption of the test liquid, sample freshness, are all parameters of the wood surface that influence on its SFE (Wålinder and Johanson 2001; Wålinder and Ström 2001). Considering all these parameters, dynamic CA analysis is therefore relevant when studying wood surfaces, since it is not limited by surface absorption and chemical heterogeneity (De Meijer et al. 2000; Gardner et al. 1991; Moghaddam et al. 2014; Petrič et al. 2013; Shen et al. 1998; Shupe et al. 1998). The result of dynamic CA measurement is a detected force in relation to time of measurement, manifested in the form of hysteresis. The recorded hysteresis is limited by advancing and receding three-phase contact line (Liptáková and Kúdela 1994; Pétrissans et al. 2003; Shen et al. 1998).

The penetration of a liquid coating into a porous woody substrate further conditions the properties of the surface system (Bastani et al. 2016). Deeper penetration ensures stronger anchoring of the coating, which improves the durability of the surface system. Both the wood and the coating influence penetration (Bessières et al. 2013; Kamke and Lee 2007; Khosravi et al. 2015; Paris and Kamke 2015). Experimentally, the penetration of a coating in the wood is usually measured at random, in sampled cross sections (Chandler et al. 2005). However, the uneven distribution of the coating into wood makes the determination of a representative coating penetration depth challenging (Van den Bulcke et al. 2003). For this reason, alternative techniques have been used to map the coating penetration in wood, such as scanning electron microscopy, and X-ray micro-computed tomography (micro-CT) (De Vetter et al. 2006; Mayo et al. 2010; Van den Bulcke et al. 2008; Van den Bulcke et al. 2010; Wascher et al. 2020).

The present work aims to quantify the interaction of a commercial waterborne coating with unmodified wood

and TM wood, wood either untreated (UT) or pre-treated with an airborne atmospheric plasma discharge. The research was focused on the influence of treatment of wood with plasma on selected properties of wood. At first, the plasma discharges' visual appearance was analysed during wood treatment with plasma. Then, the dynamic wettability of unmodified and TM wood was investigated by the Wilhelmy plate method which yielded the SFE and the dynamic coating CA. The changes in MC were recorded, assuming that the air discharge would be dependent on the presence of water. Finally, coating penetration in UT and PTd wood was studied with micro-CT.

2 Materials and methods

2.1 Wood and sample preparation

Quartersawn planks from the central part of Norway spruce (*Picea abies* (L.) Karst.) and common beech (*Fagus sylvatica* L.) logs, obtained from local forests in Slovenia, free of macroscopic defects such as knots and splits, were selected. The nominal density and MC were 561 kg•m^{-2} and 11.8% respectively for spruce wood and 713 kg•m^{-2} and 11.9% for beech wood, as determined by gravimetry. Half of these 35 mm thick planks were heat-treated in an inert atmosphere, at vacuum and temperature of 230 °C for 3 h (Rep et al. 2012). Before and after the treatment, the wood was conditioned at (103 ± 2) °C for 12 h. The planks were then cut into smaller specimens with different geometries for the different experiments. Extra care was taken to ensure that specimens shared similar annual ring widths. Before each experiment, the samples were stored in a conditioning chamber at 20 °C and 65% relative humidity (RH), for at least 7 days.

2.2 Plasma treatment (PT) process and discharge analysis

PT of the samples was performed with a custom-made device, with a dielectric barrier discharge plasma produced by a floating electrode dielectric barrier discharge (FE-DBD), that generates non–thermal plasma in air at atmospheric pressure (Žigon et al. 2019). Schematics of the set-up are shown in Figure 1. An alternating high voltage (frequency 5 kHz, 15 kV peak voltage) with sinusoidal waveform was regulated via a high voltage power supply. Plasma was ignited between the surface of the treated wood sample (moving at 2 mm·s^{-1}) and two tubular ceramic dielectrics (Al_2O_3, thickness 2.5 mm), each with a round brass electrode (15 mm diameter) inside. The distance between the dielectrics was set to 5 mm, and the distance between the dielectrics and the surface of the wood sample was 1 mm. PT was performed in a room conditioned at 20 °C and RH 50%.

To study the differences in generated plasma discharges on different substrates, pictures of the discharges were taken with a Nikon D5600 DSLR camera (aperture f/7.1, shutter speed 0.1 s, ISO sensitivity 2000). The photographed gap between the sample surface and the insulated electrode were analysed by measuring the light intensity in the Fiji software (ImageJ 1.46d, Bethesda, Maryland, USA) (Schindelin et al. 2012). A line was drawn along the discharge, and the grey values were obtained with a plot profile function.

2.3 Determination of wood mass loss through PT

Before starting the investigation of the influence of PT on wood mass, samples were stored in a chamber with an aqueous solution of saturated potassium sulphate (K_2SO_4). At 20 °C, climate conditions with a RH of 92% were established. The samples were kept in the chamber until they reached a constant MC, with a maximum of 14 days. Five samples per material type were subjected to the plasma discharge 20 times, while UT samples (5 per material) were simply maintained in dry conditions (20 °C, 30% RH). Before and after each PT iteration, the mass of the sample was measured with a precise (0.001 g accuracy) scale (PR10/98, Mettler Toledo, Columbus, OH, USA), and the relative mass loss was calculated according to Eq. (1):

$$\Delta m = 100\,\% - \frac{m_t \cdot 100\%}{m_{t0}}, \tag{1}$$

where Δm represents relative mass loss [%], m_t measured sample mass after certain number of passes through plasma discharge [g] and m_{t0} sample mass before first exposure to plasma discharge [g].

2.4 Contact angle (CA) measurements and determination of the surface free energy (SFE)

For CA measurements, 10 samples with dimensions 20 × 30 × 2 mm (radial × longitudinal × tangential, abbreviated L × R × T) were prepared from each material, following the procedures from previous studies (e.g. Petrič et al. 2007). The Wilhelmy plate method was used to estimate the apparent advancing CA of demineralized water, diiodomethane, and formamide on these samples. To prevent liquid soaking in the axial direction, the cross sections of the samples were coated with a nitrocellulose transparent varnish (Helios d.o.o., Količevo, Slovenia). Prior to measurements, the samples were stored in a conditioning chamber at 20 °C and 65% RH. The measurements were carried out at room temperature and RH with a Krüss Processor Tensiometer K100 (Krüss, Hamburg, Germany). The surface tension properties of the test liquids were obtained from Krüss LabDesk database. Each sample was used for one test cycle, firstly immersed into the liquid with the grain perpendicular to the direction of immersion, and then pulled out in reverse. The measurement started when the liquid buoyancy force acting on the sample could firstly be detected. The immersion and pull-out speed were fixed at 6 mm·min^{-1} and the force detection sensitivity was set at 0.001 N. The maximum immersion depth was 7 mm, and the measurement ended when the sample was back in its initial position. After the test cycle, both the advancing CA and the receding CA were determined by the software Krüss LabDesk.

The CA data were used for the SFE calculation of the solid surfaces by the Owens-Wendt (OWRK) method (Owens and Wendt 1969). The total surface free energy (γ_{sv}), and its two components: the polar γ_{sv}^{p} and the dispersive γ_{sv}^{d} component, could thus be determined.

In addition, the CAs of the liquid waterborne commercial acrylic coating (Belinka Interier, Belinka Belles, d.o.o., Ljubljana,

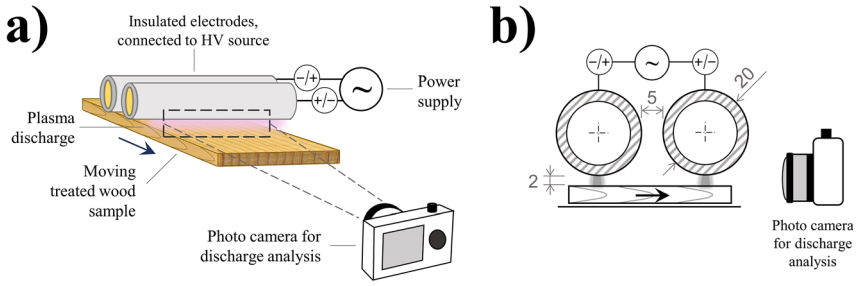

Figure 1: Schematic representation of FE-DBD plasma treatment process of wood, and photographic setup: 3D view (a) and side view with dimensions in mm (b).

Slovenia) were determined with the same procedure as the CAs of the other liquids.

2.5 Determination of coating penetration depth

2.5.1 Micro-CT scanning: One longitudinal sample of spruce and beech wood each, with dimensions 5 × 3 × 3 mm (L × R × T) was cut out of straight-grained material. Smaller dimensions of the samples enabled more precise detailed surface preparation and more precise later analysis. Both radial surfaces for coating were smoothed by cutting on a sliding microtome. One radial surface of each sample was treated with plasma, as explained in Section 2.2. Immediately after the PT, a 10 µL droplet of coating was applied with a pipette on the PTd surface. After the coating droplet had dried, another was applied with the same method, but on the UT surface. The samples were scanned before and after this coating application, using the Nanowood X-ray equipment (Dierick et al. 2014), built at the Centre for X-ray tomography at Ghent University. Scanned volumes were reconstructed with the Octopus Reconstruction software (Dierick et al. 2004), currently distributed by TESCAN-XRE, formerly known as XRE, a spin-off company of UGCT. The scans were performed at a tube voltage of 50 kV, and a target power of 5 W. 2001 projections were acquired over a 360° sample rotation. Each projection required 1 s of exposure time. The reconstructed voxel size was 2.5 µm^3, and 16 bit images were produced.

2.5.2 Image analysis: Image analysis and visualization were performed in Fiji. Upon reconstruction, volumes were median-filtered by a line structure element of half-length 5 voxels in the grain direction. To quantify the penetration depth of the coating, the 3D volumes (Figure 2) were analysed following the procedure described in Van den Bulcke et al. (2010). Firstly the volume of interest was aligned by a rotation in each Cartesian plane. Then, the coated surface (either PTd or not) was set as a base plane, from which the penetration depth could be analysed. However, due to the similarity in grey values (i.e. local X-ray absorptions), wood tissue is not distinguishable from the coating. Hence, automatic segmentation of the coating alone could not be performed. Instead, segmenting the air from solid matter (non-air voxels, comprising both the wood and the coating) was possible, which was done on a volume that was resliced in the tangential direction. The aim was to get a distribution of porosity in the tangential direction. In turn, we could deduce the presence of coating from the absence of porosity, which is an integral part of wood, but is absent in the liquid coating. The percentage of non-air voxels was obtained on each slice, i.e. every 2.5 µm in the samples depth.

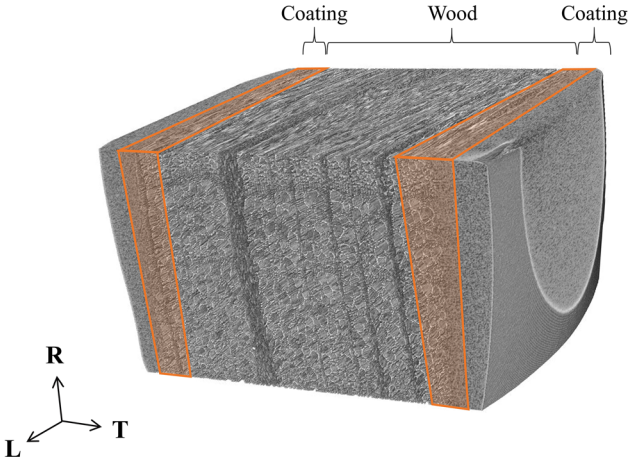

Figure 2: 3D visualisation of a beech sample after coating, and schematic representation of the image analysis. The length of the marked regions is 1 mm in tangential (T) direction.

3 Results and discussion

3.1 Discharge intensity and plasma streamers distribution

The results of the photographic experiment to capture the plasma discharges are presented in Figure 3. The light intensity during the PT of beech wood, encoded in 8 bit grey values, amounted to 20 ± 7, in arbitrary units. The light intensity during the PT of spruce wood resulted in lower intensities, i.e. 17 ± 7, about 18% lower than for beech. With TM wood, the average intensity was 12 ± 4 for beech, and 10 ± 2 for spruce. Therefore, thermal modification had a clear impact on the plasma, which was much less intense on TM wood. This correlates with the MC of a particular substrate, as this is the main parameter defining the electrical conductivity of wood (Fredriksson et al. 2013; Zelinka et al. 2008; Vermaas 1984). On TM specimens, the light intensity of the plasma discharge strongly declines with lower MC. This is probably related to the difference between cell lumen and cell wall-bound water. Indeed, the MC of wood is in constant balance with the relative

humidity of the surrounding environment. The light intensity, however, is determined by the electric and dielectric properties of the substrate, which is also dependent on the "bound water", inside cells and carbonized parts of the TM wood. In the pictures shown in Figure 3, plasma streamers are localized and intensified on the latewood areas, which had already been shown in a previous studies (Levasseur et al. 2014; Žigon and Dahle 2019). Enlarged pictures of the samples exposed to plasma discharges, and comparison of detected light intensity are given in Figure S1 and Figure S2 of the article's supplemental material (Žigon et al. 2020).

3.2 Wood mass loss during PT

In the climate chamber (20 °C, 92% RH) the samples reached the following average MCs: beech 25.6 ± 0.5%, spruce 22.2 ± 0.2%, TM beech 16.5 ± 0.2%, and TM spruce 15.4 ± 0.5%. The relative mass loss as a function of the number of PT cycles is presented in Figure 4. It can be seen that the relative mass loss increased with each pass through the plasma discharge. For each PTd sample, an UT specimen was kept in the lab and weighted accordingly. Thus, the comparison of PTd and UT specimens made it possible to account for any drying process inherent to the lab conditions. After 20 passes, the greatest mass loss was recorded for PTd beech (5.5%) and PTd spruce wood (4.7%), while exposure of the UT samples to the lab conditions induced lower loss of their initial mass (2.7 and 3.9% for spruce and beech, respectively). The mass loss of TM woods was lower than that of unmodified wood. Mass loss of PTd TM spruce was 1.5%, and 1.3% on the UT specimen. In comparison, 20 plasma exposures of TM beech wood induced a 2.7% mass loss, and a 2.2% mass loss in the UT specimen. These results relate to the MC: the higher the MC, the higher the mass loss.

Among samples, the detected differences in relative mass loss reflected the differences in their MC. The

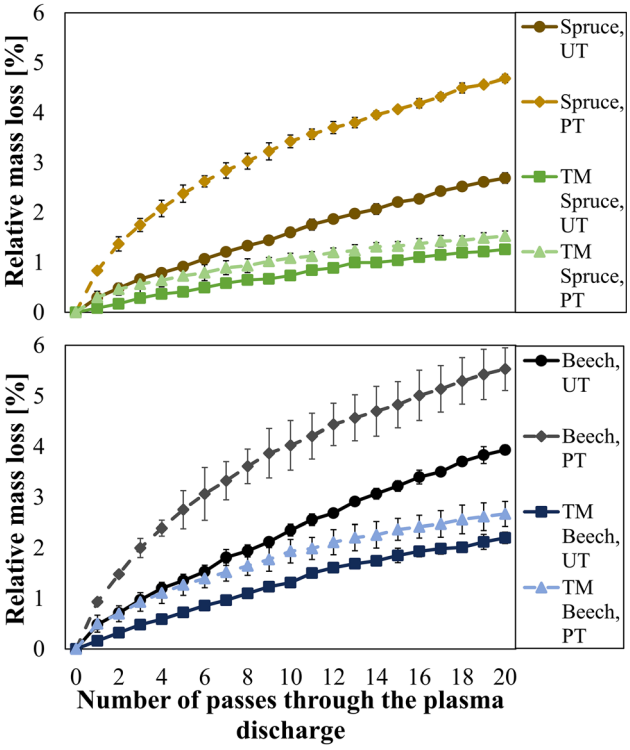

Figure 4: Relative mass loss of untreated (UT) and plasma-treated (PT) samples of unmodified and thermally modified (TM) spruce and beech, during 20 passes through the plasma discharge.

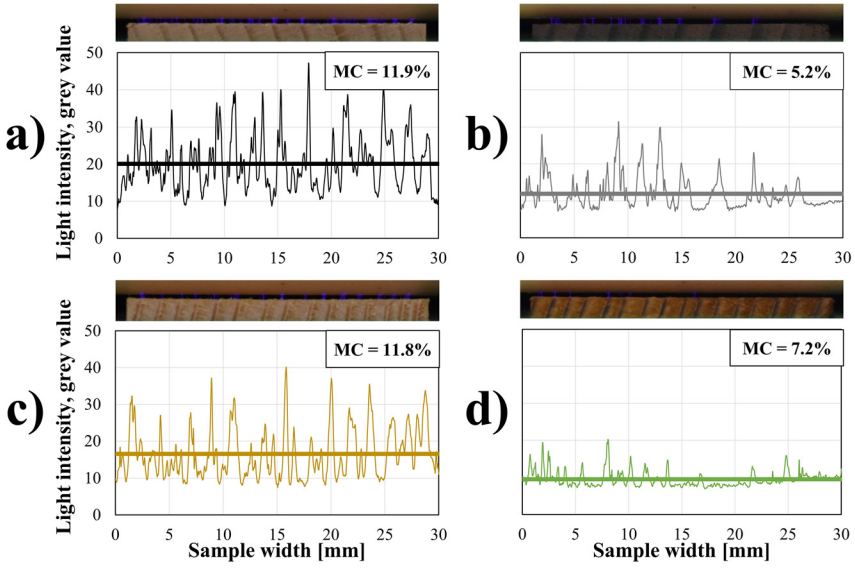

Figure 3: Distribution and average of the detected light intensity, measured in the discharge, as a function of the sample width: beech (a), TM beech (b), spruce (c), and TM spruce (d).

differences between the MC of UT samples, and the MC of PTd samples are presented in Table 1.

These findings show that PT increases water removal from wood. However, we believe that this needs confirmation with further experiments. Indeed, more complete parameter studies for initial MC, atmosphere, wood species, and PT conditions will be needed to include the observed behaviour into the general theory of drying. To the best of our knowledge, no discussion on the water evaporation from substrates during exposure to DBDs generated in atmospheric conditions was published so far. However, an increased rate of water evaporation, when exposed to an electric field, was reported by Barthakur and Arnold (1995), and Zhou and co-workers (2001), among others. In electrohydrodynamic drying (Singh 2012), the principal driving force for evaporation is an ion drag phenomenon. These ions create vortex motions in water and other surface constituents with dipole properties, when subjected to an external electric field (Relvas et al. 2015). In the literature, several studies can be found on enhanced water evaporation or drying from various materials when exposed to DBD (Hijosa-Valsero et al. 2013; Iervolino et al. 2019; Molina et al. 2014) and other plasma discharges (Buβler et al. 2017; Foster 2017; Gamaleev et al. 2019; Morshed et al. 2012; Rezaei et al. 2019; Wang et al. 2012; Zhang et al. 2019).

3.3 Calculated SFE and coating CA

SFEs were calculated from measurements of the advancing CA of three different liquids, according to the Owens-Wendt (1969) method. The results revealed that thermal modification of beech and spruce wood resulted in a decrease in SFE compared to unmodified samples (Figure 5). The reason for emphasized hydrophobic properties of wood after thermal modification, detected by dynamic CA measurements, are modifications of wood polysaccharide components and the decrease of the electron-donating component of the SFE (Gérardin et al. 2007; Hakkou et al. 2005). For all our studied materials, after thermal modification the polar component of the SFE decreased, whereas the share of the dispersive component increased. The total SFE of all materials increased after PT, to which contributed the increase of the polar part of the SFE. The positive influence of PT on increased SFE was especially visible on beech wood, and less on spruce wood. PT of TM wood only slightly increased the total SFE. However, it was mostly due to the increase of the polar part that contributes to enhanced interactions with polar liquids.

The surface tension of the acrylic coating we used was 30.1 $mN \cdot m^{-1}$, as determined in previous studies. The wetting profiles of dynamic CA, measured on 10 samples on each of 8 material variations determined with Wilhelmy plate method, are presented in Figure 6. A hysteresis is clearly visible in all cases, showing that the advancing CAs are larger than the receding ones. The wetting force defines the advancing curves. The wetting force can be impacted by surface roughness effects, chemical heterogeneity, or liquid absorption (Chibowski et al. 2002; De Meijer et al. 2000). The area of the CA hysteresis was found to be smaller in TM samples than in unmodified samples. This concurs with the reduced wettability and reduced sorption of waterborne coatings by TM woods (Pétrissans et al. 2003). However, the detected advancing coating CAs were higher at normal woods than TM woods. Similar finding was reported by Petrič and co-authors (2007). Beside the nature of the wooden substrate, the authors assigned this to a low surface tensions of the tested waterborne coating. The advancing CAs of the coating decreased after PT of the substrate, indicating its enhanced wettability. The greatest

Table 1: The difference in MC loss between untreated (UT) and plasma-treated (PTd) samples after 20 passes through the plasma discharge.

Type of wood	Loss in moisture content, %		
	UT	PTd	Difference PTd - UT
Beech	4.8 (± 0.1)	6.9 (± 0.4)	2.1 (± 0.5)
TM beech	2.7 (± 0.1)	3.0 (± 0.3)	0.3 (± 0.4)
Spruce	3.3 (± 0.1)	5.7 (± 0.1)	2.4 (± 0.2)
TM spruce	1.5 (± 0.1)	1.8 (± 0.1)	0.3 (± 0.2)

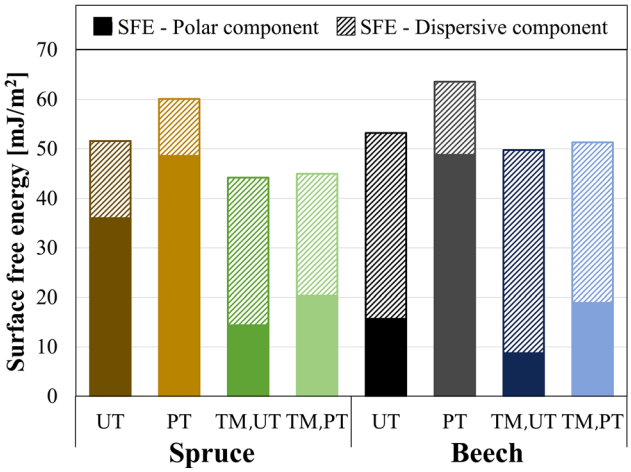

Figure 5: Calculated SFE of untreated (UT) and plasma-treated (PT) unmodified and thermally modified (TM) spruce and beech wood. The solid part of the colums represents the polar part of the SFE, while the hatched part represents the dispersive component of the SFE.

difference of the advancing CA between the UT ($\Theta_{A,\ UT}$) and PT ($\Theta_{A,\ PT}$) substrates was found at 10.3° for beech and at 8.3° for spruce. On TM specimens, these differences were less pronounced. Yet, for TM beech and TM spruce woods, the PTd samples had CAs 4.5° or 2.6° lower than UT samples, on average. Although a waterborne coating was used, the change of the coating's CA after PT seems to correlate better with the total SFE, than with the polar part of the SFE. This indicates that the dispersed acrylic phase strongly affects and determines the overall interaction between the wood and the liquid coating.

3.4 Coating penetration depth

Wetting of wood with a coating is accompanied by its specific penetration into porous structure of wood (Liptáková and Kúdela 1994). Figure 7 shows example micro-CT slices of coated beech (Figure 7a) and spruce (Figure 7b) samples. The distribution of the coating in beech tissue is more complex than in spruce, due to the more complex wood anatomy (Bastani et al. 2016).

The distribution of the average amount of non-air voxels per slice, i.e. the inverse porosity, is shown in Figure 8. The tangential distance, shown in the *x*-axis, takes the 0 as the reference where the coating was visually detected deepest in the wood. The inverse porosity is stable in the negative region of the tangential distance (–50–0 µm), meaning that the wood pores are no longer filled with a coating (hence the porosity is only resulting from the wood structure, which is roughly homogeneous in the tangential direction). This also confirms the visual identification of the deepest penetration. In this internal

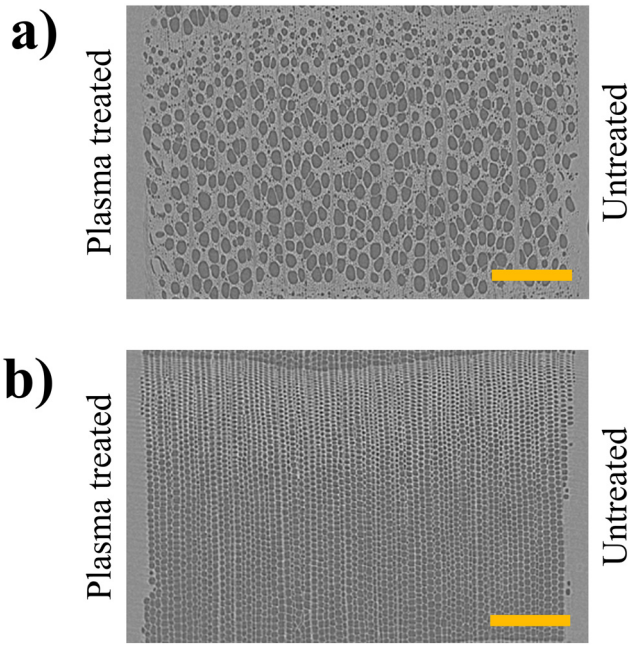

Figure 7: Example micro-CT slices in the (R–T) plane, for beech (a) and spruce (b). The scale bar represents 500 µm. The coating is visible on both sides of each slice. Examples of both wood segmentations, including the percentage of non-air voxels, are presented in the supplements, Figure S3 (Žigon et al. 2020).

region, the inverse porosity is lower in spruce [UT: (40.0 ± 1.2)% and PTd: (43.4 ± 1.4)%] than it is in beech [UT: (50.7 ± 1.6)% and PTd: (52.3 ± 1.1)%]. Of course, this is due to the lower density (i.e. higher porosity) of spruce wood (Pretzsch et al. 2018). On the other hand, the inverse porosity increases with the positive tangential distance, until it reaches saturation (100%). At this point, slices contain only coating, which unlike wood, has no porosity

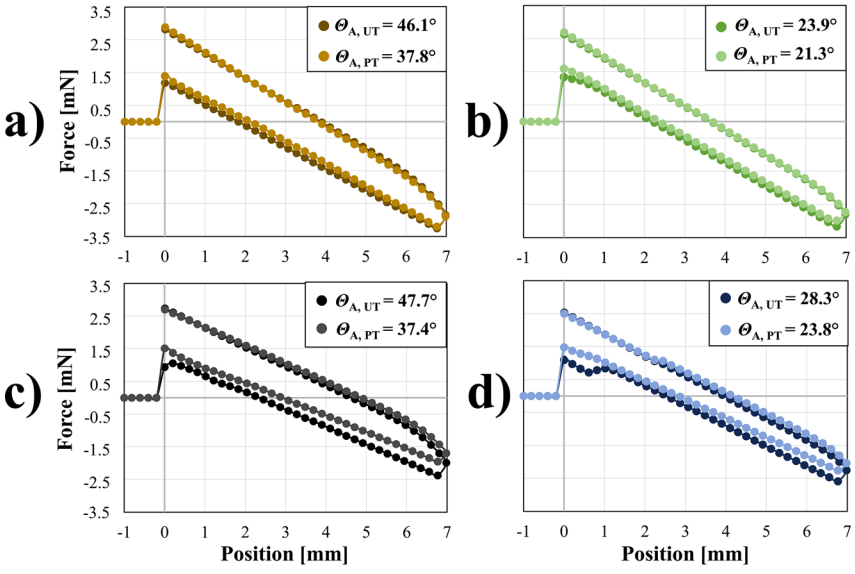

Figure 6: Detected force as a function of sample position, during the Wilhelmy plate measurements on different untreated (UT) and plasma-treated (PT) samples: unmodified spruce (a), TM spruce (b), unmodified beech (c), and TM beech (d). These samples were immersed in a waterborne acrylic coating. The measurements include the advancing CA (Θ_A).

at scanning resolution. The size of the analysed cross section for determination of inverse porosity was 29 × 31 mm at beech and 27 × 37 mm at spruce (L × R). The analysis showed that the coating penetrated deeper in beech samples than in spruce samples, as the transition region from pure wood to pure coating spans a larger tangential distance. The more heterogeneous anatomical structure of a diffuse porous beech wood, with larger cellular cavities (Bessières et al. 2013), is the predominant reason for the deeper coating penetration in beech, compared to softwoods (Bastani et al. 2016; Van den Bulcke et al. 2003).

In the beech sample, the coating penetrated the UT (290.0 µm) and PTd (297.5 µm) sides similarly. On the opposite, PT appeared to increase the coating penetration depth in spruce, since the coating was detected deeper in the PTd surface (162.5 µm) than in its UT counterpart (125.0 µm). Contrary findings between beech and spruce wood make it hard to draw a definitive conclusion, as to whether or not the PT enhances the coating penetration depth.

The PT seems to have an opposite effect on the penetration depth as it had on the SFE, particularly on the polar part of the SFE. On beech and TM beech, the polar part of the SFE tripled or doubled, respectively, but the penetration of the coating hardly changed. In contrast to that, the polar part only increased by approx. 1/3rd on both unmodified spruce and TM spruce, and the penetration increased by the same proportion. Thermal modification of beech however, made the coating penetrate much deeper already, such that the PT was not expected to also enhance the coating penetration much.

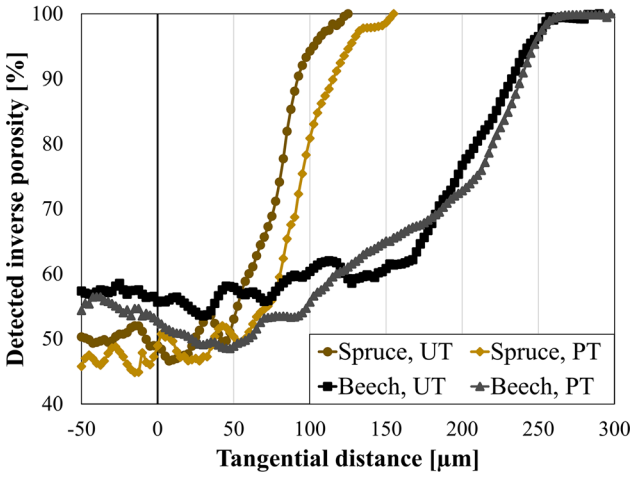

Figure 8: Inverse porosity as a function of the tangential distance in different untreated (UT) and plasma-treated (PT) substrates.

4 Conclusions

Norway spruce wood and common beech wood, either thermally modified or not, were treated with a plasma discharge generated in air at atmospheric pressure. An optical study during the treatment process showed that the distribution of formed plasma streamers was localized on denser latewood regions. Furthermore, the intensity of the discharge depended on the MC and nominal density of the treated wood, which was shown by intensity measurements of the emitted light. At all studied samples, a continuous loss of mass was detected with each pass through the plasma discharge. However, the exact correlation with the MC and structural properties of the materials has yet to be determined. The mass loss due to plasma treatment of TM woods was lower than of unmodified woods, and is correlated with the amount of water that wood contains in bulk. PT increased the total SFE of all materials studied. The increase of SFE was especially pronounced in its polar component. This was well indicated by dynamic CA measurements of a commercial waterborne coating with the Wilhelmy plate method. The increase of the SFE polar part after PT, corresponded to a decrease in values of the advancing coating CA, indicating enhanced wettability of woods with the coating. Finally, the coating distribution on untreated and plasma-treated radial surfaces, of spruce and beech wood samples, was studied with X-ray microtomography. It was shown that the span of the coating penetration was larger in beech samples than in spruce ones. The plasma treatment of the beech specimen before the coating application did not significantly influence the coating's penetration depth. However, a deeper penetration of the coating was observed in the plasma-treated surface of spruce. Nevertheless, a more generalized description will require more extensive studies involving larger number of samples. Furthermore, in-depth analyses of relation between coating penetration and anatomical features (e.g. the presence of open or closed vessels, etc.) should be added in future studies. For this purpose, nano-tomography of the contact angles between the coating and the internal wood surface (e.g. fibre or vessel walls) would be interesting.

Author contributions: All the authors have accepted responsibility for the entire content of this submitted manuscript and approved submission.

Research funding: The authors acknowledge the financial support of the Slovenian Research Agency (research core funding no. P4-0015) and the Research Foundation – Flanders (FWO) within the SBO project MoCCHa-CT

(S003418N). This project has received funding from the European Union's Horizon 2020 research and innovation programme under grant agreement no. 745936.

Conflict of interest statement: The authors declare no conflicts of interest regarding this article.

References

Altgen, D., Avramidis, G., Viöl, W., and Mai, C. (2016). The effect of air plasma treatment at atmospheric pressure on thermally modified wood surfaces. Wood Sci. Technol. 50: 1227–1241.

Altgen, D., Altgen, M., Kyyrö, S., Rautkari, L., and Mai, C. (2020). Time-dependent wettability changes on plasma-treated surfaces of unmodified and thermally modified European beech wood. Eur. J. Wood Wood Prod. 78: 417–420.

Barthakur, N.N. and Arnold, N.P. (1995). Evaporation rate enhancement of water with air ions from a corona discharge. Int. J. Biometerol. 39: 29–33.

Bastani, A., Adamopoulos, S., Koddenberg, T., and Militz, H. (2016). Study of adhesive bondlines in modified wood with fluorescence microscopy and X-ray micro-computed tomography. Int. J. Adhesion Adhes. 68: 351–358.

Bessières, J., Maurin, V., George, B., Molina, S., Masson, E., and Merlin, A. (2013). Wood-coating layer studies by X-ray imaging. Wood Sci. Technol. 47: 853–867.

Bußler, S., Ehlbeck, J., and Schlüter, O.K. (2017). Pre-drying treatment of plant related tissues using plasma processed air: impact on enzyme activity and quality attributes of cut apple and potato. Innovat. Food Sci. Emerg. Technol. 40: 78–86.

Chandler, J.G., Brandon, R.L., and Frihart, C.R. (2005). Examination of adhesive penetration in modified wood using fluorescence microscopy. In: *ASCSpring 2005 convention and exposition: April 17–20, Columbus, OH, USA*. Adhesive and Sealant Council, Bethesda, Maryland, USA, p. 10.

Chibowski, E., Ontiveros-Ortega, A., and Perea-Carpio, R. (2002). On the interpretation of contact angle hysteresis. J. Adhes. Sci. Technol. 16: 1367–1404.

Custódio, J., Broughton, J., Cruz, H., and Hutchinson, A. (2008). A review of adhesion promotion techniques for solid timber substrates. J. Adhes. 84: 502–529.

De Meijer, M., Haemers, S., Cobben, W., and Militz, H. (2000). Surface energy determinations of wood: comparison of methods and wood species. Langmuir 16: 9352–9359.

De Vetter, L., Cnudde, V., Masschaele, B., Jacobs, P.J.S., and Van Acker, J. (2006). Detection and distribution analysis of organosilicon compounds in wood by means of SEM-EDX and micro-CT. Mater. Char. 56: 39–48.

Dierick, M., Masschaele, B., and Van Hoorebeke, L. (2004). Octopus, a fast and user-friendly tomographic reconstruction package developed in LabViewR. Meas. Sci. Technol. 15: 1366–1370.

Dierick, M., Van Loo, D., Masschaele, B., Van den Bulcke, J., Van Acker, J., Cnudde, V., and Van Hoorebeke, L. (2014). Recent micro-CT scanner developments at UGCT. Nucl. Instrum. Methods B 324: 35–40.

Esteves, B.M., Domingos, I.J., and Pereira, H.M. (2008). Pine wood modification by heat treatment in air. Bioresources 3: 142–154.

Foster, J.E. (2017). Plasma-based water purification: challenges and prospects for the future. Phys. Plasmas 24:055501.

Fredriksson, M., Wadsö, L., and Johansson, P. (2013). Small resistive wood moisture sensors: a method for moisture content determination in wood structures. Eur. J. Wood Prod. 71: 515–524.

Frangi, A. and Fontana, M. (2003). Charring rates and temperature profiles of wood sections. Fire Mater. 27: 91–102.

Galmiz, O., Talviste, R., Panáček, R., and Kováčik, D. (2019). Cold atmospheric pressure plasma facilitated nano-structuring of thermally modified wood. Wood Sci. Technol. 53: 1339–1352.

Gamaleev, V., Iwata, N., Hori, M., Hiramatsu, M., and Ito, M. (2019). Direct treatment of liquids using low-current arc in ambient air for biomedical applications. Appl. Sci. 9: 3505.

Gardner, D.J., Generalla, N.C., Gunnells, D.W., and Wolcott, M.P. (1991). Dynamic wettability of wood. Langmuir 7: 2498–2502.

Gérardin, P., Petrič, M., Petrissans, M., Lambert, J., and Ehrhrardt, J.J. (2007). Evolution of wood surface free energy after heat treatment. Polym. Degrad. Stabil. 92: 653–657.

Gospodinova, D.N. and Dineff, P.D. (2019). Energy efficiency of atmospheric pressure plasma-aided porous media surface finishing. IOP Conf. Ser. Mater. Sci. Eng. 618: 6.

Gramlich, M.W., Gardner, J.D., and Neivandt, J.D. (2006). Surface treatments of wood-plastic composites (WPCs) to improve adhesion. J. Adhes. Sci. Technol. 20: 1873–1887.

Hakkou, M., Pétrissans, M., Zoulalian, A., and Gérardin, P. (2005). Investigation of wood wettability changes during heat treatment on the basis of chemical analysis. Polym. Degrad. Stabil. 89: 1–5.

Hijosa-Valsero, M., Molina, R., Schikora, H., Müller, M., and Bayona, J.M. (2013). Removal of priority pollutants from water by means of dielectric barrier discharge atmospheric plasma. J. Hazard. Mater. 262: 664–673.

Humar, M., Kržišnik, D., Lesar, B., Thaler, N., Ugovšek, A., Zupančič, K., and Žlahtič, M. (2017). Thermal modification of wax-impregnated wood to enhance its physical, mechanical, and biological properties. Holzforschung 71: 57–64.

Iervolino, G., Vaiano, V., and Palma, V. (2019). Enhanced removal of water pollutants by dielectric barrier discharge nonthermal plasma reactor. Separ. Purif. Technol. 215: 155–162.

Jamali, A. and Evans, P.D. (2011). Etching of wood surfaces by glow discharge plasma. Wood Sci. Technol. 45: 169–182.

Kamke, F.A. and Lee, J.N. (2007). Adhesive penetration in wood – a review. Wood Fiber Sci. 39: 205–220.

Khosravi, S., Nordqvist, P., Khabbaz, F., Öhman, C., Bjurhager, I., and Johansson, M. (2015). Wetting and film formation of wheat gluten dispersions applied to wood substrates as particle board adhesives. Eur. Polym. J. 67: 476–482.

Köhler, R., Sauerbier, P., Ohms, G., Viöl, W., and Militz, H. (2019). Wood protection through plasma powder deposition – an alternative coating process. Forests 10: 898. 14.

Kutnar, A., Kričej, B., Pavlič, M., and Petrič, M. (2013). Influence of treatment temperature on wettability of Norway spruce thermally modified in vacuum. J. Adhes. Sci. Technol. 27: 963–972.

Lapham, G.S., Dowling, D.R., and Schultz, W.W. (1999). In situ force-balance tensiomerty. Exp. Fluid 27: 157–166.

Levasseur, O., Profili, J., Gangwar, R.K., Naudé, N., Clergereaux, R., Gherardi, N., and Stafford, L. (2014). Experimental and modelling study of organization phenomena in dielectric barrier discharges with structurally inhomogeneous wood substrates. Plasma Sources Sci. Technol. 23:054006.

Liptáková, E. and Kúdela, J. (1994). Analysis of the wood-wetting process. Holzforschung 48: 139–144.

Liptáková, E., Kúdela, J., and Sarvaš, J. (2000). Study of the system wood – coating material I. Wood - liquid coating material. Holzforschung 54: 189–196.

Liptáková, E. and Kúdela, J. (2003). Study of the system wood – coating material. Part 2. Wood-solid coating material. Holzforchung 56: 547–557.

Lütkemeier, B., Konnerth, J., and Militz, H. (2016). Bonding performance of modified wood. Distinctive influence of plasma pretreatments on bonding strength. In: *World conference on timber engineering 2016 e-book*. Vienna University of Technology, Vienna, Austria, pp. 518–527.

Ma, X., Qiao, Z., Huang, Z., and Jing, X. (2013). The dependence of pendulum hardness on the thickness of acrylic coating. J. Coating Technol. Res. 10: 433–439.

Mantanis, G.I. and Young, R.A. (1997). Wetting of wood. Wood Sci. Technol. 31: 339–35.

Mayo, S.C., Chen, F., and Evans, R. (2010). Micron-scale 3D imaging of wood and plant microstructure using high-resolution X-ray phase-contrast microtomography. J. Struct. Biol. 171: 182–188.

Moghaddam, M.S., Claesson, P.M., Wålinder, M.E.P., and Swerin, A. (2014). Wettability and liquid sorption of wood investigated by Wilhelmy plate method. Wood Sci. Technol. 48: 161–176.

Molina, R., Jovancic, P., Vilchez, S., Tzanov, T., and Solans, C. (2014). In situ chitosan gelation initiated by atmospheric plasma treatment. Carbohydr. Polym. 103: 472–479.

Morshed, M.M., Alam, M.M., and Daniels, S.M. (2012). Moisture removal from natural jute fibre by plasma drying process. Plasma Chem. Plasma Process. 32: 249–258.

Novák, I., Sedliačik, J., Krystofiak, T., Lis, B., Popelka, A., Kleinová, A., Matyašovský, J., Jurokovič, P., and Bekhta, P. (2019). Study of wood surface pre-treatment by radio-frequency discharge plasma. Drewno 62: 81–91.

Odrášková, M., Ráhel', J., Zahoranová, A., Tiňo, R., and Černák, M. (2008). Plasma activation of wood surface by diffuse coplanar surface barrier discharge. Plasma Chem. Plasma Process. 28: 203–211.

Owens, D.K. and Wendt, R.C. (1969). Estimation of the surface free energy of polymers. J. Appl. Polym. Sci. 13: 1741–1747.

Paris, J.L. and Kamke, F.A. (2015). Quantitative wood-adhesive penetration with X-ray computed tomography. Int. J. Adhesion Adhes. 61: 71–80.

Peng, X. and Zhang, Z. (2020). Research of polypropylene (PP) decorative board surface painting used for wood product decoration and the paint film adhesion improvement by plasma. J. Adhes. Sci. Technol. 34: 246–262.

Petrič, M., Knehtl, B., Krause, A., Militz, H., Pavlič, M., Pétrissans, M., Rapp, A., Tomažič, M., Welzbacher, C., and Gérardin, P. (2007). Wettability of waterborne coatings on chemically and thermally modified pine wood. J. Coating Technol. Res. 4: 203–206.

Petrič, M., Kutnar, A., Rautkari, L., Laine, K., and Hughes, M. (2013). Influence of surface densification of wood on its dynamic wettability and surface free energy. In: Mittal, K.L. (Ed.), *Advances in contact angle, wettability and adhesion*. Scrivener Publishing LLC, Beverly, MA, USA, pp. 279–296.

Pétrissans, M., Gérardin, P., El bakali, I., and Serraj, M. (2003). Wettability of heat-treated wood. Holzforschung 57: 301–307.

Pretzsch, H., Biber, P., Schütze, G., Kemmerer, J., and Uhl, E. (2018). Wood density reduced while wood volume growth accelerated in central european forests since 1870. For. Ecol. Manage. 429: 589–616.

Ramé, E. (1997). The Interpretation of dynamic contact angles measured by the Wilhelmy plate method. J. Colloid Interface Sci. 185: 245–251.

Rehn, P., Wolkenhauer, A., Bente, M., Förster, S., and Viöl, W. (2003). Wood surface modification in dielectric barrier discharges at atmospheric pressure. Surf. Coating Technol. 174–175: 515–518.

Relvas, C., Castro, G., Rana, S., and Fangueiro, R. (2015). Characterization of physical, mechanical and chemical properties of quiscal fibres: the influence of atmospheric DBD plasma treatment. Plasma Chem. Plasma Process. 35: 863–878.

Rep, G., Pohleven, F., and Košmerl, S. (2012). Development of the industrial kiln for thermal wood modification by a procedure with an initial vacuum and commercialisation of modified Silvapro wood. In: Jones, D., Militz, H., Petrič, M., Pohleven, F., Humar, M., and Pavlič, M. (Eds.), *Proceedings, The sixth European conference on wood modification, Ljubljana, Slovenia, September:11–17*. University of Ljubljana, Biotechnical Faculty, Department of Wood Science and Technology, Ljubljana, Slovenia, pp. 17–18.

Rezaei, F., Vanraes, P., Nikiforov, A., Morent, R., and De Geyter, N. (2019). Applications of plasma-liquid systems: a review. Materials 12: 2751.

Schindelin, J., Arganda-Carreras, I., Frise, E., Kaynig, V., Longair, M., Pietzsch, T., Preibisch, S., Rueden, C., Saalfeld, S., Schmid, B., et al. (2012). Fiji – an open source platform for biological image analysis. Nat. Methods 9: 676–682.

Setoyama, K. (1996). Surface modification of wood by plasma treatment and plasma polymerisation. J. Photopolym. Sci. Technol. 9: 243–250.

Shen, Q., Nylund, J., and Rosenholm, J.B. (1998). Estimation of the surface energy and acid-base properties of wood by means of wetting method. Holzforschumg 52: 521–529.

Shi, S.Q. and Gardner, D.J. (2001). Dynamic adhesive wettability of wood. Wood Fiber Sci. 33: 58–68.

Shupe, T.E., Hse, C.Y., Choong, E.T., and Groom, L.H. (1998). Effect of wood grain and veneer side of loblolly pine veneer wettability. For. Prod. J. 46: 95–97.

Singh, A., Orsat, V., and Raghavan, V. (2012). A comprehensive review on electrohydrodynamic drying and high-voltage electric field in the context of food and bioprocessing. Dry. Technol. 30: 1812–1820.

Sun, Z., Guanben, D., and Linrong, H. (2009). Effect of microwave plasma treatment on surface wettability of common teak wood. Front. For. China 4: 249–245.

Surini, T., Charrier, F., Malvestio, J., Charrier, B., Moubarik, A., Castéra, P., and Grelier, S. (2012). Physical properties and termite durability of maritime pine Pinus pinaster Ait, heat-treated under vacuum pressure. Wood Sci. Technol. 46: 487–501.

Talviste, R., Galmiz, O., Stupavská, M., Tučeková, Z., Kaarna, K., and Kováčik, D. (2019). Effect of DCSBD plasma treatment on surface properties of thermally modified wood. Surf. Interfaces 16: 8–14.

Tjeerdsma, B.F., Boonstra, M., Pizzi, A., Tekely, P., and Militz, H. (1998). Characterisation of the thermally modified wood: molecular reasons for wood performance improvement. Holz Roh- Werkstoff 56: 149–153.

Van den Bulcke, J., Rijckaert, V., Van Acker, J., and Stevens, M. (2003). Quantitative measurement of the penetration of water-borne

coatings in wood with confocal laser microscopy and image analysis. Holz Roh- Werkstoff 61: 304–310.

Van den Bulcke, J., Masschaele, B., Dierick, M., Van Acker, J., Stevens, M., and Van Hoorebeke, L. (2008). Three-dimensional imaging and analysis of infested coated wood with X-ray submicron CT. Int. Biodeterior. Biodegrad. 61: 278–286.

Van den Bulcke, J., Boone, M., Van Acker, J., and Van Hoorebeke, L. (2010). High-resolution X-ray imaging and analysis of coatings on and in wood. J. Coating Technol. Res. 7: 271–277.

Vermaas, H.F. (1984). The influence of sample density on the D.C. resistance of wood. Holzforschung 38: 109–112.

Wascher, R., Bittner, F., Avramidis, G., Bellmann, M., Endres, H.J., Militz, H., and Viöl, W. (2020). Use of computed tomography to determine penetration paths and the distribution of melamine resin in thermally-modified beech veneers after plasma treatment. Compos Part A. Appl. Sci. Manuf. 132: 105821.

Wang, R.X., Nian, W.F., Wu, H.Y., Feng, H.Q., Zhang, K., Zhang, K., Zhu, W.D., Becker, K.H., and Fang, J. (2012). Atmospheric-pressure cold plasma treatment of contaminated fresh fruit and vegetable slices: inactivation and physiochemical properties evaluation. Eur. Phys. J. D 66: 276.

Wålinder, M.E.P. and Gardner, D.J. (1999). Factors influencing contact angle measurements on wood particles by column wicking. J. Adhes. Sci. Technol. 13: 1363–1374.

Wålinder, M.E.P. and Johansson, I. (2001). Measurement of wood wettability by Wilhelmy method. Part 1. Contamination of probe liquids by extractives. Holzforschung 55: 21–32.

Wålinder, M.E.P., and Ström, G. (2001). Measurement of wood wettability by Wilhelmy method. Part 2. Determination of apparent contact angles. Holzforschung 55: 33–41.

Wålinder, M.E.P. (2002). Study of lewis acid-base properties of wood by contact angle analysis. Holzforschung 56: 363–371.

Welzbacher, C.R. and Scheiding, W. (2011). Implementation of a quality assurance system for thermally modified timber (TMT) by the association of central european TMT-producers. In: *The international research group on wood protection, 11-40558*. IRG/WP: Stockholm, Sweden.

Willems, W., Lykidis, C., Altgen, M., and Clauder, L. (2015). Quality control methods for thermally modified wood. Holzforschung 69: 875–884.

Wilhelmy, J. (1863). Über die Abhängigkeit der Kapillaritäts-Konstanten des Alkohols von Substanz und Gestalt des Benetzten Festen Körpers. Ann. Phys. 119: 177–217.

Wolkenhauer, A., Avramidis, G., Hauswald, E., Militz, H., and Viöl, W. (2009a). Sanding vs. plasma treatment of aged wood: a comparison with respect to surface energy. Int. J. Adhesion Adhes. 29: 18–22.

Wolkenhauer, A., Avramidis, G., Hauswald, E., Loose, S., and Viöl, W. (2009b). Investigation on the drying behaviour of adhesives on plasma-treated wood materials. Wood Res. 54: 59–66.

Zelinka, S.L., Glass, S.V., and Stone, D.S. (2008). A percolation model for electrical conduction in wood with implications for wood–water relations. Wood Fiber Sci. 40: 544–552.

Zhang, X.-L., Zhong, C.-S., Mujumdar, A.S., Yang, X.-H., Deng, L.-Z., Wang, J., and Xiao, H.-W. (2019). Cold plasma pretreatment enhances drying kinetics and quality attributes of chili pepper (Capsicum annuum L.) J. Food Eng. 241: 51–57.

Zhou, J., Liu, Z., She, P, and Ding, F. (2001). Water removal from sludge in a horizontal electric field. Dry. Technol. 19: 627–638.

Žigon, J., Petrič, M., and Dahle, S. (2018). Dielectric barrier discharge (DBD) plasma pretreatment of lignocellulosic materials in air at atmospheric pressure for their improved wettability: a literature review. Holzforschung 72: 979–991.

Žigon, J. and Dahle, S. (2019). Improvement of plasma treatment efficiency of wood and coating process by sodium chloride aqueous solutions. Proligno 15: 260–267.

Žigon, J., Petrič, M., and Dahle, S. (2019). Artificially aged spruce and beech wood surfaces reactivated using FE-DBD atmospheric plasma. Holzforschung 73: 1069–1081.

Žigon, J., Pavlič, M., Kibleur, P., Van den Bulcke, J., Petrič, M., Van Acker, J., and Dahle, S. (2020). Supplemental material to manuscript "Treatment of wood with atmospheric plasma discharge: study of the treatment process, dynamic wettability and interactions with a waterborne coating". Zenodo, (Version 2.0.0) [Data and figures], Available at: https://doi.org/10.5281/zenodo. 4046078.

Supplementary Material: The online version of this article offers supplementary material (https://doi.org/10.1515/hf-2020-0182).